Neuro-Oncology Advances
4(1), 1–13, 2022 | https://doi.org/10.1093/noajnl/vdab182 | Advance Access date 11 December 2021

The dominant TP53 hotspot mutation in *IDH*-mutant astrocytoma, R273C, has distinctive pathologic features and sex-specific prognostic implications

Daniel F. Marker, Sameer Agnihotri, Nduka Amankulor, Geoffrey H. Murdoch, and Thomas M. Pearce

Department of Pathology, University of Pittsburgh School of Medicine, Pittsburgh, Pennsylvania, USA (D.F.M., G.H.M., T.M.P.); Department of Neurological Surgery, University of Pittsburgh School of Medicine, Pittsburgh, Pennsylvania, USA (S.A.); Department of Neurosurgery and Brain Tumor Center, Abramson Cancer Center, The University of Pennsylvania, Philadelphia, PA, USA (N.A.)

Corresponding Author: Thomas M. Pearce, MD, PhD, Department of Pathology, University of Pittsburgh School of Medicine, S701 Scaife Hall, 3550 Terrace Street, Pittsburgh, PA 15261, USA (pearcetm@upmc.edu).

Abstract

Background. Infiltrative astrocytic tumors with and without isocitrate dehydrogenase (IDH) mutation frequently contain mutations in the *TP53* tumor suppressor gene. Disruption of normal p53 protein activity confers neoplastic cells with a number of oncogenic properties and is a common feature of aggressive malignancies. However, the high prevalence of *TP53* mutation and its pathogenic role in IDH-mutant (IDHmut) astrocytoma is not well understood.

Methods. We performed a retrospective analysis of molecular and clinical data from patients with IDHmut astrocytoma at the University of Pittsburgh Medical Center between 2015 and 2019 as our initial cohort. We validated and expanded our findings using molecular and clinical data from The Cancer Genome Atlas.

Results. We show that the *TP53* mutational spectrum in IDHmut astrocytomas is dominated by a single hotspot mutation that codes for the R273C amino acid change. This mutation is not enriched in IDH-wildtype astrocytomas. The high prevalence of $TP53^{R273C}$ mutation is not readily explained by known mutagenic mechanisms, and $TP53^{R273C}$ mutant tumors have lower transcriptional levels of proliferation-related genes compared to IDHmut astrocytomas harboring other forms of mutant p53. Despite lower proliferation, $TP53^{R273C}$ mutant tumors tend to progress more quickly and have a shorter overall survival than those with other *TP53* mutations, particularly in male patients.

Conclusions. Our findings suggest that compared to other TP53 mutations, IDHmut astrocytomas may select for $TP53^{R273C}$ mutations during tumorigenesis. The genotype, sex, and mutation-specific findings are clinically relevant and should prompt further investigation of $TP53^{R273C}$.

Key Points

- $TP53^{R273C}$ is a highly enriched hotspot mutation specifically in IDHmut astrocytoma.
- IDHmut astrocytomas with $TP53^{R273C}$ have different gene expression profiles than those lacking this mutation.
- Despite lower expression of proliferation-related genes, these tumors have worse prognosis.

Importance of the Study

Despite decades of work, the role of *TP53* alteration in tumorigenesis remains incompletely understood. Our study has identified a single *TP53* gene mutation (R273C) that accounts for 20–30% of all *TP53* gene mutations in IDH-mutant astrocytoma. Such a high prevalence of a single *TP53* mutation has not been seen in other tumor types. Moreover, IDH-mutant astrocytoma with $TP53^{R273C}$ have sex dependent altered gene expression and overall poorer prognosis when compared to IDH-mutant astrocytomas with other *TP53* alterations. These clinical findings are not accounted for by known mutagenic mechanisms and suggest that the hypothesized ability of certain *TP53* mutations to impart gain-of-function properties in tumorigenesis may play a clinical role in IDH-mutant astrocytoma, laying the foundation for future functional studies.

Diffusely infiltrating gliomas are the most common primary malignant neoplasm of the central nervous system (CNS) and exhibit high morbidity and mortality. Curative therapeutic strategies for these tumors remain elusive.[1,2] Despite the overall grim prognosis, a wide spectrum of biologic behavior exists among this category of tumors, ranging from the relatively indolent course of low-grade neoplasms to the much more aggressive glioblastoma (GBM). The distinctive patterns of molecular alterations that drive the initiation and progression of these neoplasms are increasingly recognized as a critical determinant of tumor behavior, and the World Health Organization (WHO) now formally incorporates molecular findings into the glioma classification scheme.[3] Under this system, the isocitrate dehydrogenase (IDH)-mutant astrocytoma is recognized as a specific diagnostic entity, distinct from all other tumors of astrocytic lineage. Compared to their IDH-wild type (IDHwt) counterparts, astrocytomas with mutations in the *IDH1* or *IDH2* gene (IDHmut) tend to occur in younger patients, have a lower histologic grade at presentation, and have an improved prognosis.

The large majority of IDHmut astrocytomas of all grades harbor two additional molecular characteristics: *TP53* gene mutations, identified in over 90% of tumors, and inactivating mutations of the *ATRX* gene, identified in over 70% of tumors.[4–6] In contrast to events such as *CDKN2A* deletion that often occur later in the evolution of disease, the changes in *TP53* and *ATRX* are early driver-type events, the ubiquity of which suggests they play an essential role in initiating and maintaining tumor growth. The high prevalence of *TP53* mutation during early gliomagenesis in this relatively less aggressive neoplasm is especially curious, as other *TP53*-mutated tumors of the brain and other anatomic locations typically exhibit highly malignant behavior.

The markedly elevated rate of *TP53* mutations found in IDHmut astrocytoma is not identified in most other glial tumors, nor in non-CNS neoplasms driven by *IDH1/2* mutations. In the IDHwt diffuse astrocytic tumor category, a substantially smaller subset of tumors (<30%) also acquire *TP53* mutations, and unlike IDHmut tumors, these tend to present with higher histologic grade, have a more aggressive clinical course, and may acquire the *TP53* mutation later in tumor evolution.[3,7–9] In oligodendroglioma, which shares both glial origins and IDH mutation, *TP53* mutations are quite rare (<3%).[4–6] Likewise, of the non-CNS tumors that harbor mutant IDH, including subsets of leukemia, cholangiocarcinoma, and chondrosarcoma, none seem to require *TP53* mutation as an early driver event.[10,11] In fact, *TP53* mutation is rare in IDHmut cholangiocarcinoma, occurring at far lower frequency than in IDHwt cholangiocarcinoma.[12] These comparisons suggest that mutant p53 plays a uniquely critical role in IDHmut astrocytoma, for reasons unrelated to either IDH mutation or glial lineage alone.

Previous studies have suggested that different subsets of *TP53* mutations might have differential relevance in certain subtypes of glioma. Using largely outdated categories that separated GBMs into primary (*de novo*) and secondary (arising from lower-grade gliomas), it was observed that secondary GBMs harbored a higher rate of certain hotspot *TP53* mutations than primary GBMs.[13,14] With the introduction of the molecular-driven classification scheme in 2016, we now know that the vast majority of secondary GBMs represent IDHmut tumors. Given these findings, we hypothesized that the specific *TP53* mutational spectra of IDHmut and IDHwt astrocytomas may differ considerably, and that the characterization of such differences could provide unique insight into the pathogenesis of both diseases.

Methods and Materials

Cohort Descriptions

Diffusely infiltrating glioma specimens from the University of Pittsburgh Medical Center (UPMC) archives were identified (UPMC cohort). Data were collected from specimens that underwent molecular analysis by the GlioSeq™ next-generation sequencing panel between 2015 and 2019. Details on the GlioSeq panel can be found in the Supplementary Methods. 668 infiltrating astrocytic tumors were identified, of which 108 were IDHmut. Demographic data, diagnosis, and grade were collected from the surgical pathology reports. Blinded re-review of histologic slides was performed by two neuropathologists (DFM and TMP), confirming diagnosis and WHO grade in all cases. Ki67 was estimated to the nearest percent in the area of highest proliferation. These estimates were largely concordant with the originally reported value in the pathology report, with the exception of an apparent typographical error in one original report. One case (tumor 19) did not have a Ki67-stained

slide available for review, and the originally reported value was used. All data were collected with the approval of the University of Pittsburgh Institutional Review Board (study numbers PRO07010097 and STUDY20040135). Detailed data for the UPMC cohort including patient demographic information, tumor characteristics, details of molecular alterations, and survival status and intervals, are available in Supplementary Table 1.

Additional cases were identified from The Cancer Genome Atlas (TCGA) lower-grade glioma (LGG) and GBM datasets (TCGA cohort). Clinical outcome and molecular data were downloaded from cBioPortal (https://cbioportal.org, last accessed 10/13/2020) and the NIH Genomic Data Commons (https://portal.gdc.cancer.gov/, last accessed 10/13/2020). All tumors were reclassified based on IDH and 1p/19q status to reflect current diagnostic categories.

Exclusion Criteria

For analyses comparing different *TP53* mutations, samples classified as astrocytomas by absence of 1p/19q codeletion but lacking pathogenic *TP53* mutation were excluded (UPMC cohort: 12 of 108, 11%; TCGA cohort: 11 of 160, 7%).

Data Processing and Statistical Analysis

The Python 3 programming language was used for data processing and statistical analyses. The specific packages are provided in the Supplementary Methods.

TP53 Mutation Spectrum Analysis

The frequency of various *TP53* mutations was compared by codon position using jsProteinMapper.[15] In-frame insertions and deletions and frame-shift mutations are plotted at the position of the first altered codon.

Mutational Signature Analysis

COSMIC mutational signatures (v3.1, GRCh37) for single base substitutions (SBS) were downloaded from https://cancer.sanger.ac.uk/signatures/downloads/ (accessed 2/5/2021). Signatures were derived as previously described.[16]

Methylation Analysis

Methylation data for the TCGA cohort were obtained as previously described.[17] Processed methylation data were downloaded from the NIH genomic data commons portal. Methylation sites on sex chromosomes were excluded. Dimensionality reduction via t-distributed Stochastic Neighbor Embedding (t-SNE) was performed using the implementation included in the *scikit-learn* Python package.

Gene Expression Profiling

Level 3 gene expression data were downloaded from TCGA data coordination center. This dataset shows the gene-level transcription estimates as log2(x+1) transformed RSEM normalized count. Genes are mapped onto the human genome coordinates using UCSC Xena HUGO probeMap. Differential expression analysis was performed using the LIMMA (Linear Methods for Microarray Analysis[18]) module of the WebMeV analysis platform (http://mev.tm4.org, last accessed 6/17/2020). The resulting rank-ordered gene lists were subjected to Gene Set Enrichment Analysis (GSEA) to identify significantly up- and down-regulated hallmark gene sets.[19]

Comutation Analysis

Molecular alterations identified by next-generation sequencing of the UPMC cohort were extracted from the pathology report. To allow a direct comparison between the TCGA and UPMC cohorts, mutation and copy number alteration data for the TCGA cohort was limited to those genes included in the GlioSeq[20] panel plus *CDK4*, a frequently altered gene in IDHmut gliomas that is not included in GlioSeq. Of note, the version of GlioSeq used during this time period did not distinguish between homozygous and hemizygous/complex *CDKN2A* deletion (for additional explanation, see Supplementary Methods). Data exploration and visualization was performed with the interactive browser-based widget jsComut.[15] The TCGA cohort contained only a small number (15) of IDHmut, TP53-mutant glioblastomas, of which only 1 harbored a $TP53^{R273C}$ mutation, making it unsuitable for comparative analyses with the UPMC cohort.

Immunohistochemistry

Immunohistochemical staining of formalin fixed, paraffin embedded (FFPE) tissue sections was performed at the UPMC clinical laboratory as part of routine diagnostic evaluation of all cases in the UPMC cohort. Additional details can be found in the Supplementary Methods.

Survival Analysis

Survival status and date of death/last known alive for patients in the UPMC cohort was determined from the electronic medical record and publicly searchable online sources. Survival intervals were measured from the date of initial pathologic diagnosis. Subsequent specimens demonstrating tumor progression to a higher WHO grade were used to calculate progression-free intervals. Survival status and interval for the TCGA cohort were downloaded directly from the TCGA. Kaplan–Meier survival curves, log-rank statistical testing, and multivariate Cox-Proportional Hazards (Cox-PH) analysis were performed using the *lifelines* Python module.

Results

TP53 Mutational Profile Depends Critically on IDHmut Status

We first examined whether IDHmut and IDHwt astrocytomas had distinct TP53 mutational profiles, as

was suggested by previous comparisons of primary versus secondary GBM[13] and GBM versus lower-grade gliomas.[14] Using the interactive browser-based visualization tool jsProteinMapper,[15] we explored the distribution of mutations along the *TP53* gene, with cases stratified by WHO grade and IDH status (Figure 1A). A striking finding emerged: IDHmut astrocytomas of all grades showed a single dominant hotspot at codon 273 which accounted for 38% of all *TP53* mutations, whereas IDHwt tumors showed a broader, more conventional mix of mutations that more closely resembled the pan-cancer mutation profile, with 4.8% of mutations occurring at codon 273 ($P < .001$, chi-squared test). To corroborate this observation made on the UPMC cohort, we turned to the TCGA LGG and GBM datasets, and observed the same findings, with codon 273 accounting for a much higher proportion of all *TP53* mutations than any other hotspot, in IDHmut but not IDHwt astrocytomas (21% vs 5.3%, $P < .01$, chi-squared test).

R273C is the Only Dominant TP53 Hotspot Mutation in IDHmut Astrocytomas

Mutations at codon 273 can lead to multiple possible amino acid changes depending on the nucleotide-level alteration (Figure 2A). Two of these, R273H and R273C, are considered hotspot mutants across all cancers, each accounting for ~2.5–3% of all *TP53* mutations across cancer subtypes.[21,22] To determine whether the dominant codon 273 hotspot in IDHmut astrocytomas was due to one or both of these possible mutations, we next examined the specific frequencies of each possible hotspot amino acid change (Figure 1B and C). Notably, only the R273C amino acid change was highly enriched, while R273H showed a similar frequency to the other unenriched hotspot mutations. This is not a common phenomenon: across all TCGA studies, the only organ with highly imbalanced frequencies of these two mutations is the brain (Figure 3A).

Examination of the mutational spectra across patient demographics revealed that R273C mutations were more common in females versus males, to varying degrees. In the UPMC cohort the R273C mutation accounted for 34% of all *TP53* mutations in females and 27% in males, though this was not statistically significant. In the TCGA data set, the difference was more marked, with R273C accounting for 26% of mutations in females versus 11% in males ($P < .05$, chi-squared test).

Enrichment of the TP53^{R273C} Mutation is Not Explained by Known Mutational Signatures

We first considered whether the high prevalence of *TP53*^{R273C} might be due to a particular mechanism of mutagenesis that favors this mutation over other *TP53* mutations. A selective mechanism of mutation might also explain why IDHmut astrocytomas are also highly enriched for the *IDH1*^{R132H} mutation compared other functionally equivalent IDH mutations.[23,24] To examine this possibility, we turned to the emerging literature of mutational signatures in human cancers, in which mutagenic mechanisms are identified by the patterns of base substitutions that result from different causes of unrepaired DNA damage.[16,25] *TP53*^{R273C} and *IDH1*^{R132H} both occur due to cytosine (C) to thymidine (T) transitions (C>T) at methylated CpG sites, as do other oncogenic mutations at *TP53* codons 273 and 175 and *IDH1* codon 132, which are pan-cancer hotspots but not highly enriched in IDHmut astrocytoma (Figure 2A and B). Since C>T transitions are highly represented in certain COSMIC single base substitution (SBS) signatures (eg clock-like signature 1), we asked whether the trinucleotide context (TC) of the highly enriched versus nonenriched mutations might match any of these previously identified signatures. To plausibly explain the frequencies at which *TP53*^{R273C} and *IDH1*^{R132H} are found in IDHmut astrocytomas, the TCs of these mutations (ie GCG or ACG) would need to account for a reasonable proportion of all mutations within candidate signatures. We identified four signatures in which one of these TCs exceeded 5% of all mutations (SBS1, SBS6, SBS15, SBS87). Of these, SBS6 and SBS15 would favor transitions causing *TP53*^{R273C} over *TP53*^{R273H} and *IDH1*^{R132H} over *IDH1*^{R132C}, recapitulating the enrichments seen in clinical samples (Figure 2C). Two lines of evidence argue against these signatures being a sufficient explanation, however. First, the *TP53*^{R175H} hotspot mutation has the same GCG TC as *TP53*^{R273C} yet is not equivalently enriched. Second, the profile of base transitions of all other noncodon-273 *TP53* mutations is not a good match (Figure 2D), and it is implausible that mutagenic mechanisms would preferentially act only at specific codons of a gene.

Molecular Characteristics of TP53^{R273C}-Mutant Astrocytomas Versus Those with Other TP53 Mutations

We next hypothesized that the high prevalence of *TP53*^{R273C} mutations within IDHmut astrocytomas could arise from selective advantage, and asked whether *TP53*^{R273C} mutant tumors have different molecular characteristics than those harboring other types of mutant p53 protein. Several possible mechanisms exist. Given the critical epigenetic remodeling effects of mutant IDH, we wondered whether *TP53*^{R273C} mutation might systematically affect the tumor methylome. However, *TP53*^{R273C} mutant tumors did not form a distinct methylation cluster, as visualized by t-SNE dimensionality reduction (Figure 3B). Excluding IDHwt and oligodendroglioma samples from the analysis did not substantially change this distribution (not shown). Additional methylation-based analyses also failed to segregate these tumors – the global methylation levels in *TP53*^{R273C} mutant tumors versus others were not different, and *TP53*^{R273C} tumors showed no significant predilection for either the glioma CpG island methylator (G-CIMP) -low or -high methylation clusters.[17,26]

We then investigated the possibility that *TP53*^{R273C} preferentially produces dominant-negative mutant p53 protein (ie not necessitating loss of the wild-type allele), reasoning that this could provide a selective advantage to transformed precursor cells during early gliomagenesis. To answer this, we took advantage of the ubiquity of IDH mutations in all tumor cells and the allelic heterozygosity necessary for tumor cell survival and D-2HG oncometabolite

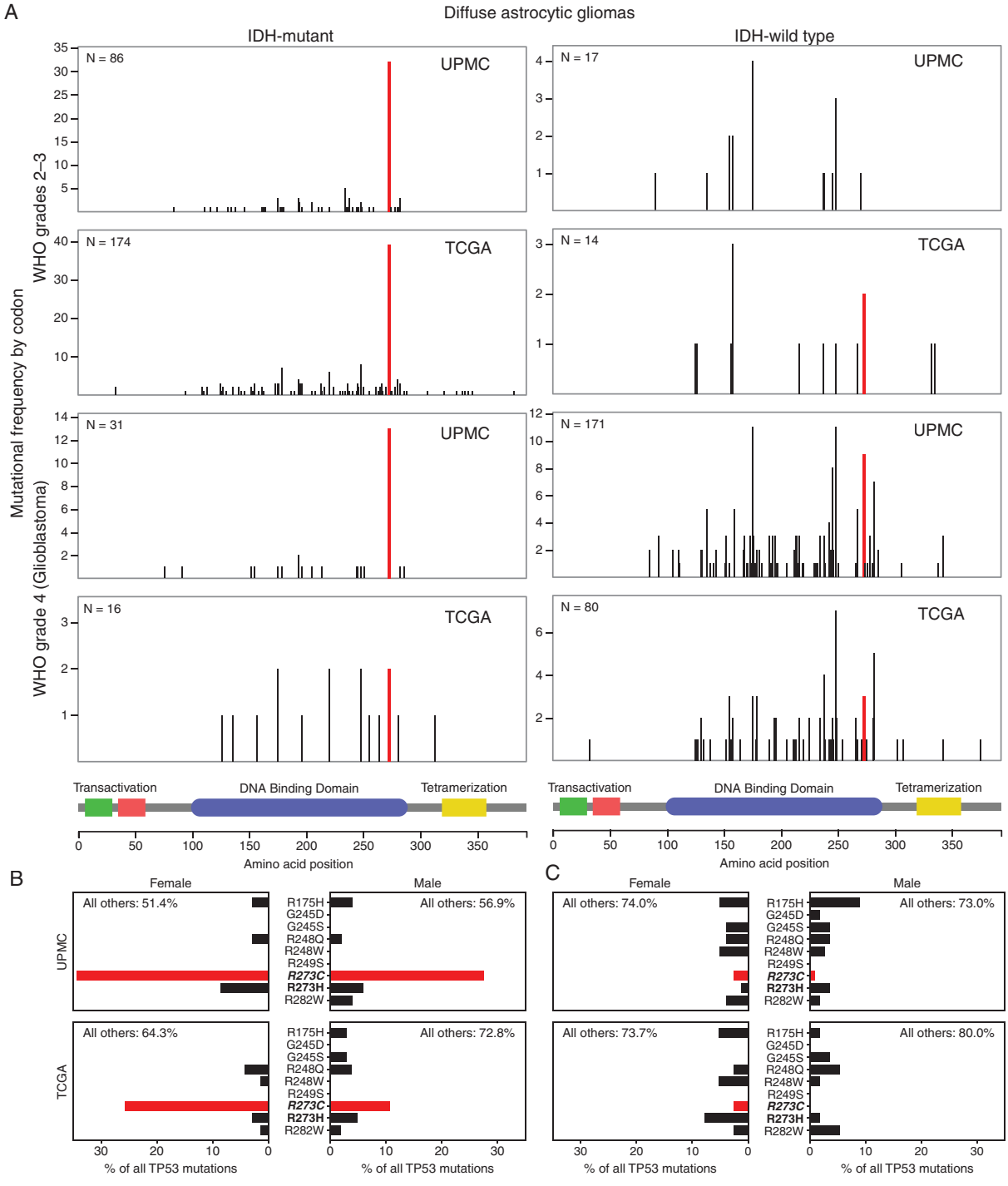

Figure 1. R273C is the single dominant *TP53* hotspot mutation in IDHmut but not IDHwt astrocytomas. (A) *TP53* mutational profiles of IDHmut (left column) and IDHwt (right column) astrocytomas reveal a dominant hotspot at codon 273 which is specific to the IDHmut tumor subset. Note that y-axes are scaled per-plot to clearly show the distributions. (B) Mutations at *TP53* codon 273 in IDHmut astrocytomas are dominated by the R273C amino acid change, which occurs at a far higher frequency than other pan-cancer hotspot mutations, including R273H. (C) In contrast, IDHwt astrocytomas are not enriched for this mutation.

production, which provides a reference measure of tumor cellularity.[10,27–30] Leveraging this, we compared the variant allele frequency (VAF) of each *TP53* mutation to the VAF of the *IDH1/2* mutation in the same tumor (Figure 3C). Concordant with recent analyses that have demonstrated frequent (>90%) loss of the wild type p53 allele across all

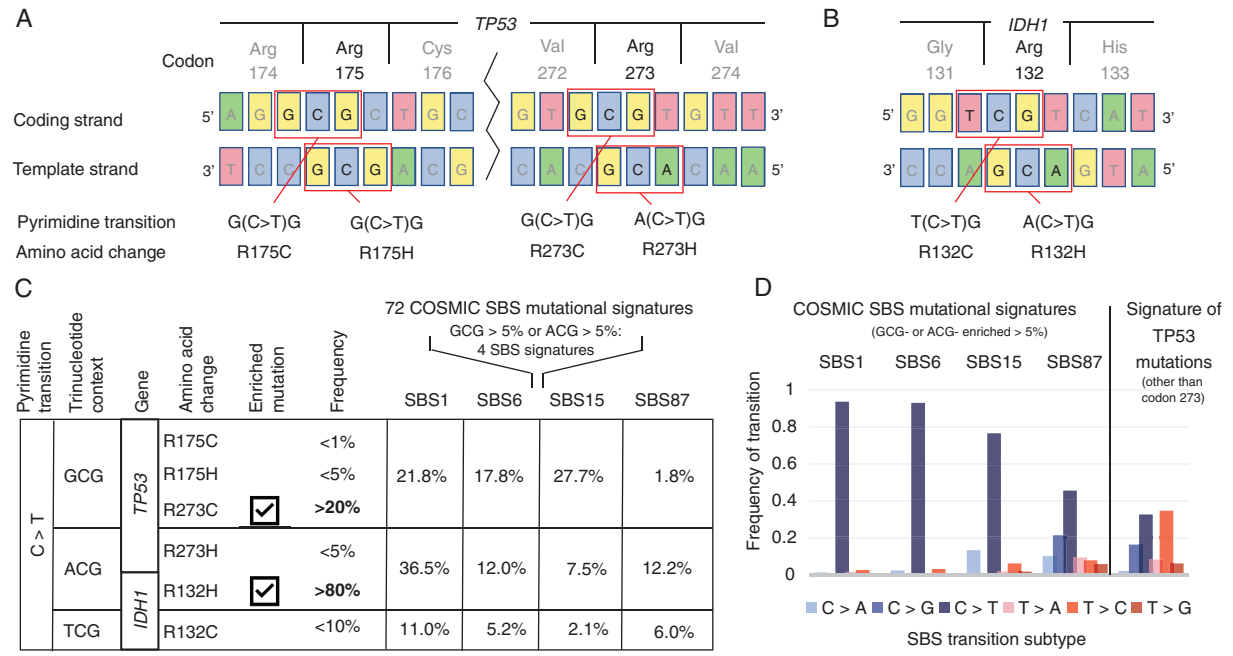

Figure 2. Enrichment of TP53^{R273C} is not accounted for by known mutational mechanism signatures. (A–B) DNA context of select point mutations at hotspot codons in *TP53* (A) and *IDH1* (B). (C) Consequences of C>T transitions at methylated CpG site at these codons, grouped by trinucleotide context. At right, the frequency at which each trinucleotide is found within the four COSMIC SBS mutational signatures that are enriched for the G(C>T)G or A(C>T)G transitions (corresponding to *TP53*^{R273C} and *IDH1*^{R132H} respectively). (D) The profile of *TP53* mutations in IDH-mutant astrocytomas does not match these SBS signatures (UPMC cohort). To avoid confounding effects, mutations at the dominant hotspot codon 273 are excluded.

cancer subtypes,[31] we find that nearly all tumors show loss of the wild type *TP53* allele: the *TP53*:*IDH1/2* VAF ratio is ~2:1 in most cases, with only a handful of tumors falling near the unity line that indicates heterozygous *TP53* mutation. Importantly, none of the *TP53*^{R273C} mutant tumors retained a wild-type allele, arguing against this possible selective mechanism.

Examining the landscape of molecular alterations seen in IDHmut astrocytomas stratified by sex and *TP53*^{R273C} mutation status (Figure 4), we found a small but statistically significant interaction between the R273C mutation and sex, as was hinted at by the increased frequency of this mutation in female patients. First considering WHO grades 2 and 3 tumors (Figure 4A) in the combined UPMC and TCGA cohorts, we found that female tumors harboring *TP53*^{R273C} showed fewer additional genomic alterations beyond the canonical IDH-TP53-ATRX triad than those with alternative *TP53* mutations, while the relationship was opposite in males (Figure 3C; $P < .05$, chi-squared test). Turning to the smaller set of IDHmut GBMs, we found that by this stage in tumor evolution virtually all tumors had acquired additional genomic hits, regardless of *TP53*^{R273C} status (Figure 4B). However, a notable difference was identified in the pattern of cooccurring alterations in GBMs, with the *TP53*^{R273C} mutants having a lower rate of *CDKN2A* copy number loss compared to tumors lacking a *TP53*^{R273C} mutation (Figure 3D; $P < .01$, chi-squared test), an important genomic event that correlates with more aggressive clinical behavior in IDHmut astrocytomas.[32–35]

Histologic Features of TP53^{R273C} Mutant Astrocytomas

Supplementary Figure S1 reviews the histopathologic features of the *TP53*^{R273C}-mutant astrocytomas. Low-grade *TP53*^{R273C} mutant tumors frequently demonstrated an oligodendroglioma-like morphology, with monotonous round nuclei and variable cytoplasmic clearing in FFPE tissue sections stained with hematoxylin and eosin (H&E; Supplementary Figure S1A). p53 immunostaining was often indeterminate (Supplementary Figure S1B-D). In addition, the Ki67 proliferation index for p53^{R273C}-mutant tumors in female patients tended to be lower compared to cases lacking this mutation, grade for grade (Supplementary Figure S1E), though this did not reach statistical significance ($P > .05$, Mann–Whitney U-test). Taking advantage of the fact that the clinical data for the TCGA LGG cohort includes the initial histologic (premolecular) diagnosis of each tumor at the time of case submission, we also found that IDHmut astrocytomas with *TP53*^{R273C} mutation were diagnosed most frequently as the now-obsolete "oligoastrocytoma," while tumors harboring other forms of mutant p53 were most commonly diagnosed as "astrocytoma" (Supplementary Figure S1F).

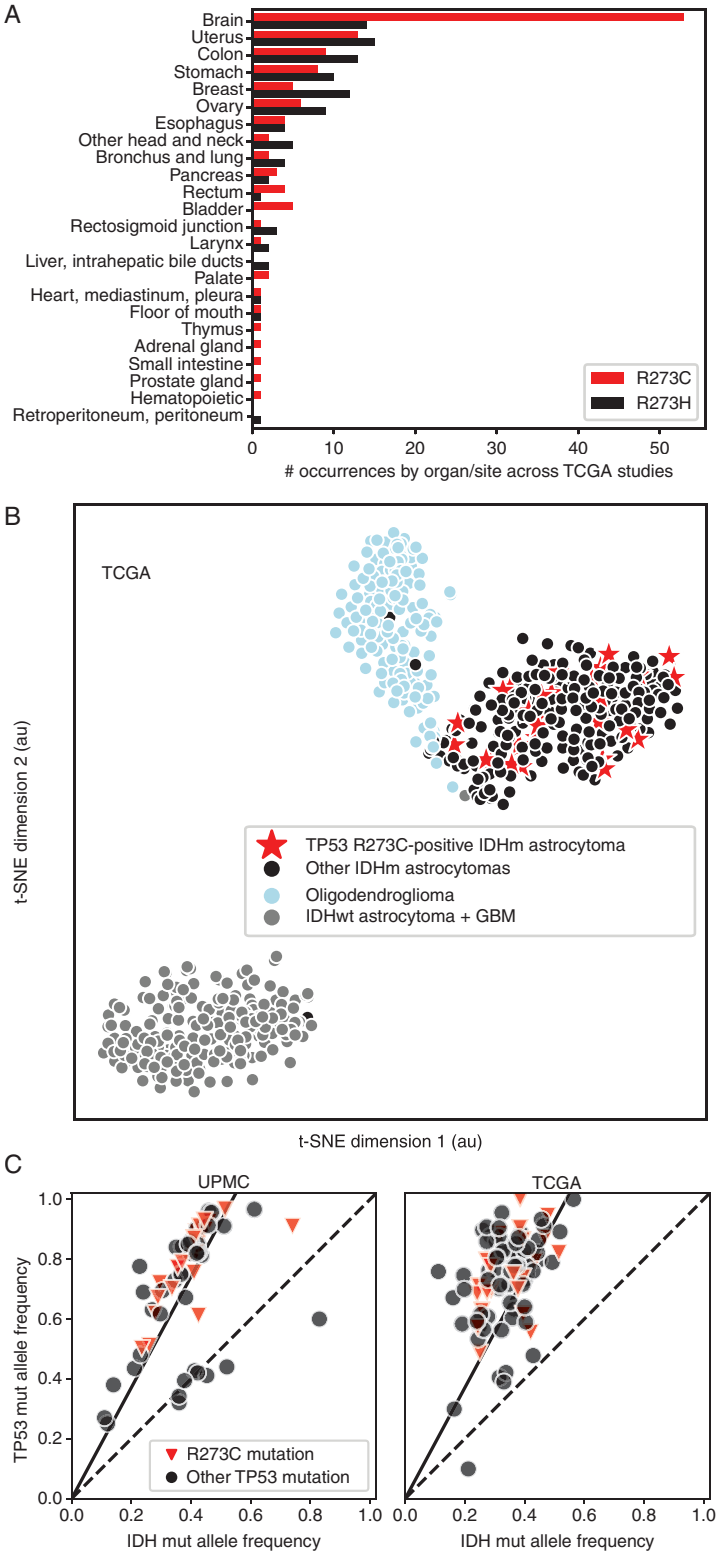

Figure 3. ***TP53*^{R273C} mutant tumors are overrepresented in brain tumors but are not different than other *TP53* mutants in DNA methylation or heterozygosity.** (A) Across all TCGA studies, *TP53*^{R273C} is seen at much higher frequency than *TP53*^{R273H} specifically in brain tumors. (B) Analysis of genome-wide methylation patterns of the TCGA cohort shows that IDHmut astrocytomas with the *TP53*^{R273C} mutation do not form a distinct cluster, but are distributed through the methylation space shared by other IDHmut astrocytomas. (C) For tumors with a single *TP53* mutation, *TP53* variant allele frequency (VAF) is plotted against the corresponding *IDH1/2* VAF.

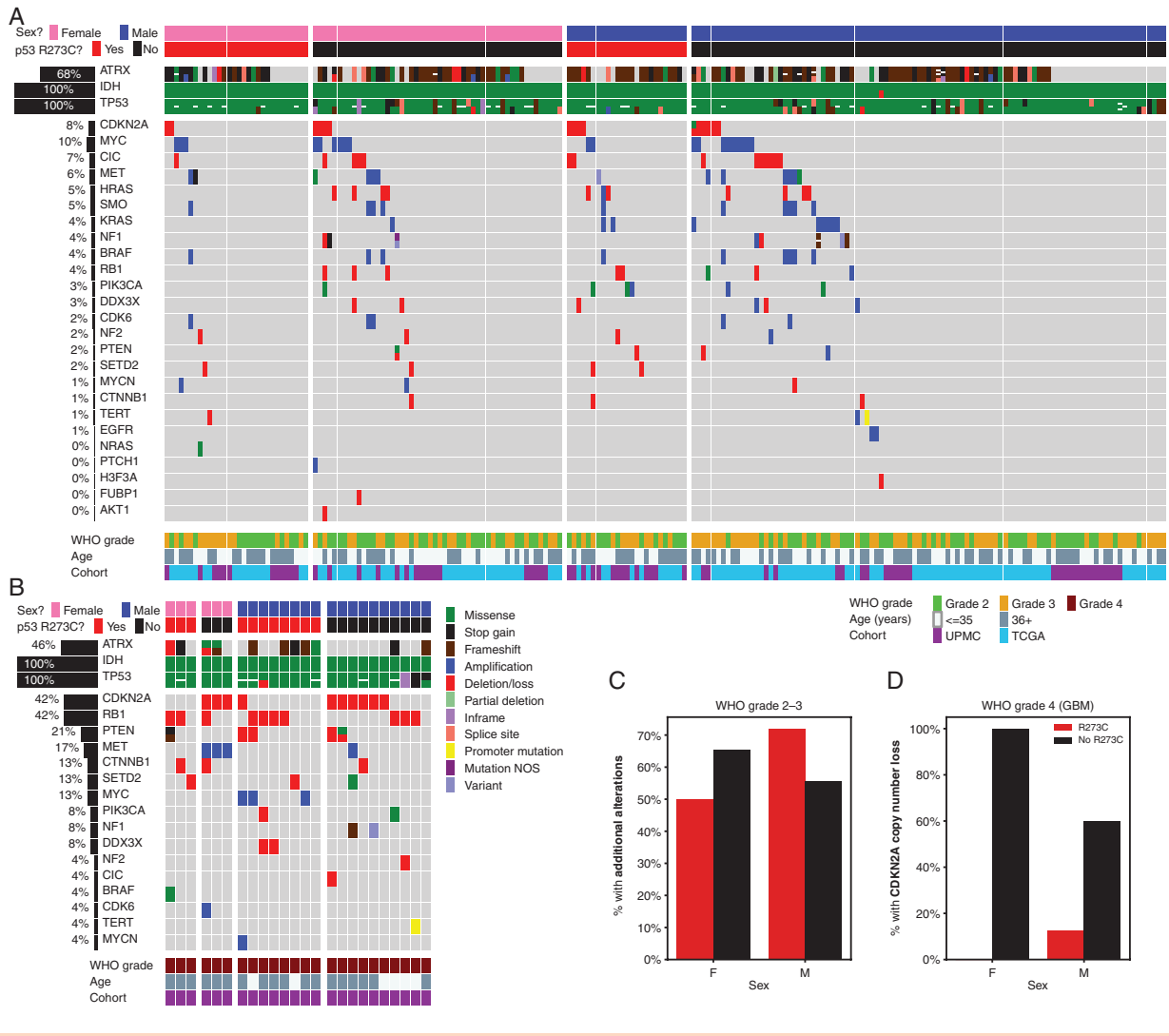

Figure 4. Comutation analysis of *TP53*^{R273C} mutants and tumors with other *TP53* mutations. (A–B) The genomic landscape of IDHmut astrocytomas, grouped by sex and *TP53*^{R273C} status, for WHO grades 2-3 (A) and WHO grade 4 (B) tumors. (C) Fewer female tumors with *TP53*^{R273C} have additional genomic alterations than those with other *TP53* mutations; this pattern is reversed in male tumors ($P < .05$, chi-squared test). (D) *TP53*^{R273C} mutant WHO grade 4 tumors show lower incidence of *CDKN2A* copy number loss than those with other *TP53* mutations ($P < .01$, chi-squared test); *RB1* loss is more common (see (B)).

Sex-Dependent Gene Expression Differences in TP53^{R273C} Mutants Versus Other TP53 Mutants

We next examined gene expression profiles for potential differences in these tumors compared to those with other *TP53* mutations. Because of the sex difference in mutational frequency, our initial differential expression analyses were dominated by genes encoded on sex chromosomes, leading us to stratify patients by sex for further analyses. Differential expression and gene set enrichment analysis revealed significant associations between the *TP53*^{R273C} mutation and gene expression, and an interaction with sex. Most strikingly, the Hallmark gene sets associated with proliferation and cell cycle, including the G2M checkpoint, E2F targets, and mitotic spindle gene sets, are downregulated in *TP53*^{R273C} mutants tumors compared to *TP53* mutations at other codons (Figure 5A and B), supporting the observation of lower Ki67 immunohistochemical labeling (Supplementary Figure S1E). This effect was larger and more statistically significant in females, but was also present in males. Since *TP53*^{R273C} is known to have a minor amount of residual binding capacity at the p53 response element,[36] we next asked whether direct p53 target genes,[37] or genes in the Hallmark p53 pathway, were differentially expressed in these tumors. Only a modest effect was seen, arguing against residual wild type function playing a significant role (Figure 5C). Notably, expression of *CDKN1A* (p21) was increased in *TP53*^{R273C} tumors specifically in females, but not males. The single most significantly up-regulated Hallmark gene set in *TP53*^{R273C} tumors is TNF-α signaling via NF-κB, which was similarly seen only seen in female tumors (Figure 5D).

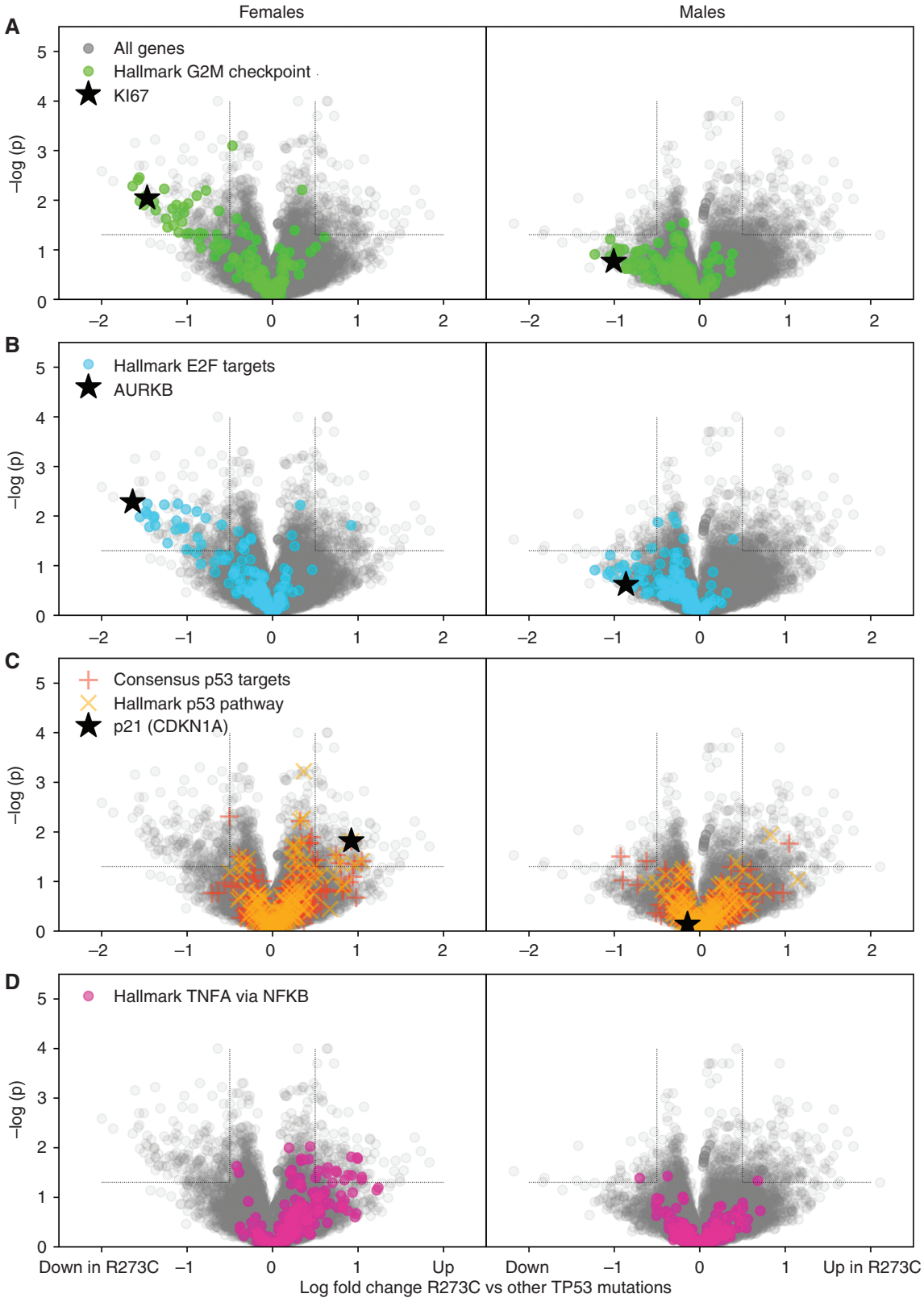

Figure 5. ***TP53*^{R273C} -mutant tumors show differential gene expression relative to other *TP53* mutations, with sex-specific differences.** LIMMA analysis of RNA expression data from the TCGA LGG cohort was used to compare gene expression in *TP53*^{R273C} astrocytomas to those lacking a codon 273 mutation. (A–B) Analysis of female tumors (left column) and male tumors (right column) demonstrates a cloud of

Given the possibility that R273H, the other hotspot mutation at codon 273, might show similar effects to R273C, we performed differential expression analysis in two stages. Data shown in Figure 5 are a comparison of R273C mutants versus *TP53* mutations at codons other than 273. We then directly compared R273C to R273H, and found the same pattern of differential expression (albeit noisy and not statistically significant due to the very small number of R273H-mutant tumors in the data set; not shown), arguing that the effect is due to the specific amino acid change, not just the codon position.

TP53^{R273C} Mutation-Specific Effects on Survival

In light of the bland morphology and decreased proliferative signature of the *TP53*^{R273C} mutant tumor subset, we wondered this molecular alteration might confer a better prognosis than other *TP53* mutations. We instead found the opposite (Figure 6 and Supplementary Figure S2). Stratifying tumors by *TP53*^{R273C} status, we find that lower-grade (grades 2-3) tumors with this mutation have shorter progression-free survival (PFS) and overall survival (OS), driven by significantly worse outcomes in male patients (Figure 6, bottom row). In the subset of tumors presenting as GBM, OS was shorter for *TP53*^{R273C} mutant tumors, though numbers are small (N = 14) and this did not reach significance (Supplementary Figure S2). Additionally, *TP53*^{R273C} approached significance in multivariate Cox-PH analyses for both PFS (P = .06–.08) and OS (P = .13–.23) with a hazard ratio of 1.63-2.59 (UPMC cohort; Supplementary Table 2).

Discussion

Recognition of the importance of mutations in the *IDH1* or *IDH2* genes on the natural history of diffuse gliomas has been a defining advance in our understanding of glioma biology over the past decade. Pathogenic IDH mutations exclusively occur at the active site of the isocitrate dehydrogenase enzyme and lend the mutant protein the neomorphic ability to catalyze NADPH-dependent reduction of α-ketoglutarate to D-2-hydroxyglutarate (D-2HG).[10] The resulting accumulation of D-2HG promotes a state of DNA and histone hypermethylation, leading to the CpG island methylator phenotype, a block of differentiation, and a host of oncogenic properties which have been extensively reviewed in the literature.[10,27,28] How this abnormal cellular state interacts with the other characteristic molecular alterations in the two subcategories of IDHmut glioma are less clear. In particular, the high frequency of missense *TP53* mutations in IDHmut astrocytoma is well described but lacking in explanation.

The existence of hotspot point mutations in *TP53* has been recognized for decades, with codons 175, 245, 248, 249, 273, and 282 accounting for a much higher frequency of all point mutations compared to all other codons.[22] Across cancers, each of these hotspot codons accounts for approximately 3–7% of the total point mutations; although 3–7% is far lower than the prevalence of single hotspot mutations in certain known oncogenes (eg *BRAF*^{V600E}), this degree of enrichment is nonetheless highly significant, and mutations at these codons are frequently hypothesized to confer beneficial gain-of-function (GOF) properties.[22,38,39] Given this baseline pan-cancer level of hotspot mutational frequencies, it is remarkable that in IDHmut astrocytomas the R273C amino acid change accounts for 20–30%+ of all *TP53* mutations.

Somatic mutations in cancer can become enriched by two primary mechanisms: selective mutagenesis or selective advantage. We find both possibilities intriguing. Currently established signatures of mutagenic mechanisms do not appear to adequately explain the pattern of highly enriched *TP53* and *IDH1* hotspot mutations in IDHmut astrocytomas (Figure 2), but it remains possible that an as-yet unidentified mutational mechanism might be active in IDHmut gliomagenesis. However, we believe the selective advantage hypothesis is more likely, as multiple lines of evidence support the idea that mutant p53^{R273C} protein may have unique effects on the tumor cell properties. At the level of gene expression, *TP53*^{R372C} mutant tumors show differential downregulation of proliferation-related gene sets compared to tumors harboring other *TP53* mutations, and upregulation of other gene sets, in a sex-dependent manner (Figure 5). The downregulation of proliferation-related gene sets is supported by lower Ki67 proliferation rates in these tumors, particularly in female patients (Supplementary Figure S1E). The frequency of additional molecular alterations also appears to subtly depend on *TP53*^{R273C} status (Figure 4), though further analysis of larger cohorts is needed. Finally, there were notable clinical differences in patients with *TP53*^{R273C} mutated astrocytomas, including increased prevalence in female patients (Figure 1B) and shorter survival, particularly in male patients (Figure 6). In light of the latter, we note that the apparent increased frequency of *TP53*^{R273C} in female patients may in part be related to the combination of longer survival of females with this mutation and the cross-sectional nature of the cohorts, which may bias the observed incidence of the mutation.

Despite tens of thousands of publications spanning decades of research on *TP53*, this "guardian of the genome" continues to generate controversy and challenge understanding.[40–42] While the high frequency of point mutations compared to truncating and deletion mutations is unquestioned, the relative contributions of GOF and dominant negative effects towards the oncogenic properties of *TP53* mutation remains contentious.[22,43–45] A recent study of *TP53* mutations in myeloid malignancies performed a detailed multi-modality investigation of the role of mutant *TP53* in these cancers.[43] The authors showed that the mutational

down-regulated genes, more prominent in females, which gene set enrichment analysis showed to be composed of proliferation-related pathways. (C) Direct p53 target genes and the Hallmark p53 pathway gene set showed modest effects, mainly in females, including significant upregulation of p21. (D) The largest up-regulated Hallmark gene set is TNF-α signaling via NF-κB.

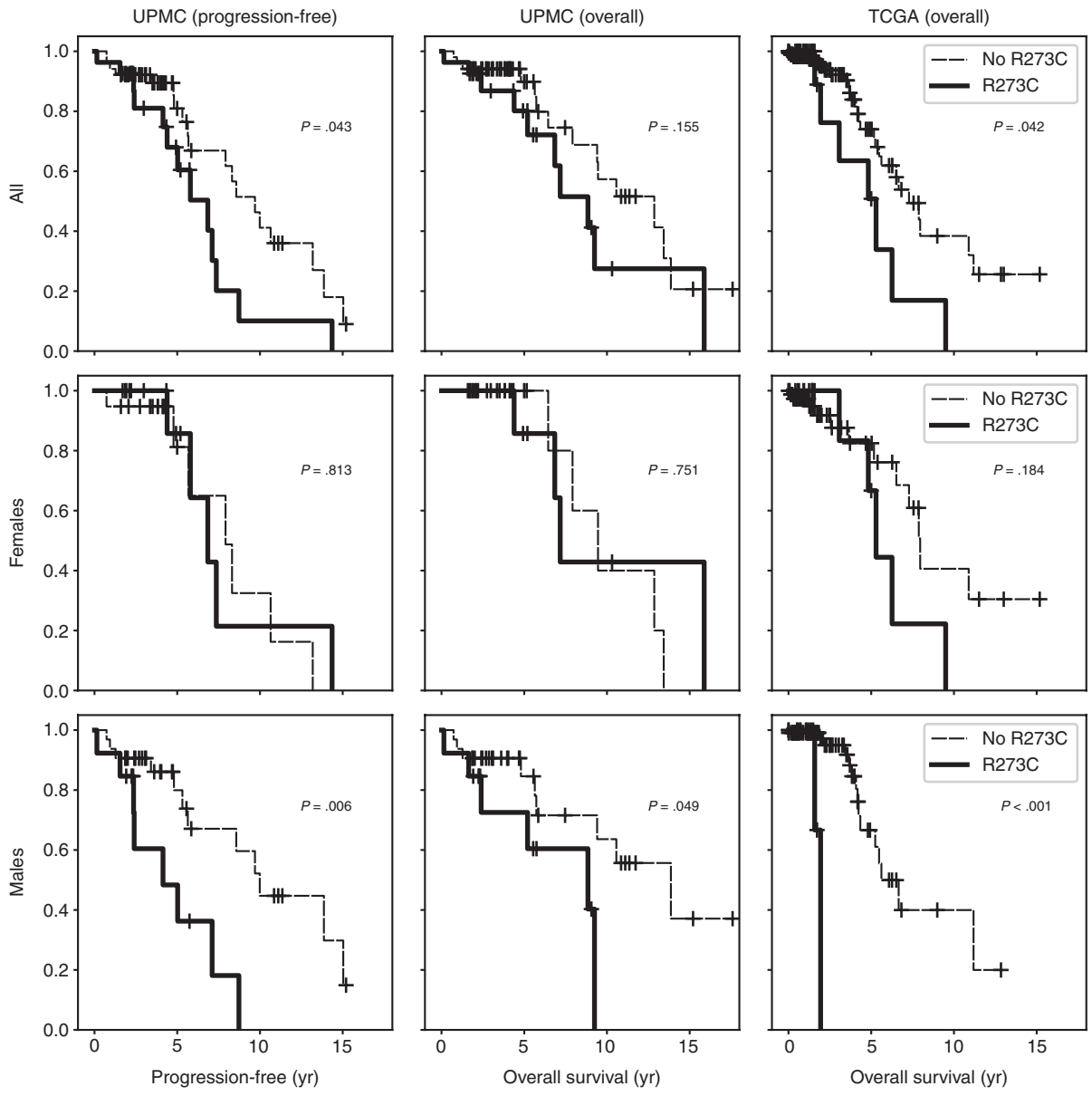

Figure 6. ***TP53*^{R273C} confers poor prognosis compared to other *TP53* mutations.** Kaplan–Meier curves for WHO grades 2–3 tumors were constructed for progression-free (UPMC) and overall survival (UPMC and TCGA). Progression includes transformation to higher WHO grade and death. *P*-values were calculated using the log-rank test.

spectrum in myeloid lesions was similar to the pan-cancer spectrum, and that the most common mutations showed no evidence of GOF activity, but rather were seemingly selected for by dominant negative mechanisms. Notably, *TP53*^{R273C} was not among the mutations studied in detail, as it was not highly prevalent in myeloid cancers. In contrast, this mutation is extremely prevalent in IDHmut astrocytomas, and tumors harboring this form of mutant p53 protein versus others appear to have a worse prognosis.

Although the precise mechanisms by which *TP53*^{R273C} differs from other *TP53* mutations in IDHmut astrocytoma are not clear from the clinical data, some possibilities appear more likely than others. The downregulation of proliferative pathways (Figure 5A and B) could indicate preservation of some degree of wild-type activity, but this is argued against by the lack of significant differential expression of other p53 target gene pathways (Figure 5C) as well as the loss of the wild-type allele in all *TP53*^{R273C} tumors (Figure 3B and C). The biology of IDHmut astrocytomas is fundamentally shaped by the G-CIMP related epigenomic remodeling caused by IDH mutation. Although *TP53*^{R273C} mutant tumors are not distinctive in DNA methylation signature (Figure 3B), an interaction with epigenetic mechanisms may occur at the level of the histone. In particular, differential interactions of p53^{R273C} with sex chromosome encoded histone demethylases could potentially explain the differing tumor behavior in male and female patients with astrocytomas containing this mutation. Another

intriguing possibility is that *TP53*^{R273C} may differentially activate NF-κB related mechanisms (Figure 5D), as this signaling pathway has been implicated in a variety of aggressive glioma phenotypes including invasiveness and therapy resistance.[46] We note, however, that significant activation of this pathway was only seen in female patients and therefore does not address the particularly poor prognosis in male patients. Experimental investigations of these hypotheses, and other possible mechanisms, would be of great interest.

In this study, we have shown that the *TP53* mutation spectrum in IDHmut but not IDHwt astrocytoma is dominated by a single highly enriched hotspot mutation, *TP53*^{R273C}. Survival analysis demonstrates mutation-specific poor outcome, particularly in male patients, despite histologic and transcriptomic evidence of lower proliferation. Intriguingly, sex-related differences identified in the UPMC and TCGA cohorts raise the possibility that *TP53*^{R273C} may have different oncogenic mechanisms and/or therapeutic responses depending on the patient's sex; it will be of great interest whether additional cohorts will further support these findings. Unfortunately, cell line and animal models of *TP53* GOF properties have focused on other hotspot mutations and largely ignored *TP53*^{R273C}. Based on our results, it seems likely that experimental work focused on *TP53*^{R273C} in IDHmut astrocytoma, in both male and female model systems, has high potential for elucidating mechanisms of p53 GOF, astrocytoma oncogenesis, and sex differences in glioma biology. Incorporation of molecular findings into brain tumor classification systems has already enabled greater diagnostic and prognostic precision. Our findings here suggest that it may be wise, at least in some cancers, to consider that specific *TP53* mutations may have distinctive properties, as we work to provide ever-more personalized medical care to patients.

Supplementary Material

Supplementary material is available at *Neuro-Oncology Advances* online.

Keywords

astrocytoma | IDH | p53 | *TP53*

Funding

No funding source supported this study.

Acknowledgments

Preliminary findings were presented at the 2019 American Association for Neuropathologists annual meeting.

Conflict of interest statement. The authors declare no conflict of interest.

Authorship statement: Study design: TMP and GHM. Analysis and interpretation: TMP, GHM, SA, NA, and DFM. Writing and revision: TMP, GHM, SA, NA, and DFM.

References

1. Shergalis A, Bankhead A 3rd, Luesakul U, Muangsin N, Neamati N. Current challenges and opportunities in treating Glioblastoma. *Pharmacol Rev.* 2018; 70(3):412–445.
2. Rajesh Y, Pal I, Banik P, et al. Insights into molecular therapy of glioma: current challenges and next generation blueprint. *Acta Pharmacol Sin.* 2017; 38(5):591–613.
3. Louis DN, Perry A, Reifenberger G, et al. The 2016 World Health Organization classification of tumors of the central nervous system: a summary. *Acta Neuropathol.* 2016; 131(6):803–820.
4. Cerami E, Gao J, Dogrusoz U, et al. The cBio cancer genomics portal: an open platform for exploring multidimensional cancer genomics data. *Cancer Discov.* 2012; 2(5):401–404.
5. Gao J, Aksoy BA, Dogrusoz U, et al. Integrative analysis of complex cancer genomics and clinical profiles using the cBioPortal. *Sci Signal.* 2013; 6(269):pl1.
6. Suzuki H, Aoki K, Chiba K, et al. Mutational landscape and clonal architecture in grade II and III gliomas. *Nat Genet.* 2015; 47(5):458–468.
7. Brennan CW, Verhaak RG, McKenna A, et al.; TCGA Research Network. The somatic genomic landscape of glioblastoma. *Cell.* 2013; 155(2):462–477.
8. Draaisma K, Chatzipli A, Taphoorn M, et al. Molecular evolution of IDH wild-type glioblastomas treated with standard of care affects survival and design of precision medicine trials: a report from the EORTC 1542 study. *J Clin Oncol.* 2020; 38(1):81–99.
9. Berzero G, Di Stefano AL, Ronchi S, et al. IDH-wildtype lower grade diffuse gliomas: the importance of histological grade and molecular assessment for prognostic stratification. *Neuro Oncol.* 2021; 23(6):955–966.
10. Cairns RA, Mak TW. Oncogenic isocitrate dehydrogenase mutations: mechanisms, models, and clinical opportunities. *Cancer Discov.* 2013; 3(7):730–741.
11. Dang L, Jin S, Su SM. IDH mutations in glioma and acute myeloid leukemia. *Trends Mol Med.* 2010; 16(9):387–397.
12. Su L, Zhang X, Zheng L, Wang M, Zhu Z, Li P. Mutation of isocitrate dehydrogenase 1 in cholangiocarcinoma impairs tumor progression by inhibiting isocitrate metabolism. *Front Endocrinol (Lausanne).* 2020; 11:189.
13. Ohgaki H, Dessen P, Jourde B, et al. Genetic pathways to glioblastoma: a population-based study. *Cancer Res.* 2004; 64(19):6892–6899.
14. Kastenhuber ER, Lowe SW. Putting p53 in Context. *Cell.* 2017; 170(6):1062–1078.
15. Pearce TM, Nikiforova MN, Roy S. Interactive browser-based genomics data visualization tools for translational and clinical laboratory applications. *J Mol Diagn.* 2019; 21(6):985–993.
16. Alexandrov LB, Kim J, Haradhvala NJ, et al.; PCAWG Mutational Signatures Working Group; PCAWG Consortium. The repertoire of mutational signatures in human cancer. *Nature.* 2020; 578(7793):94–101.

17. Ceccarelli M, Barthel FP, Malta TM, et al.; TCGA Research Network. Molecular profiling reveals biologically discrete subsets and pathways of progression in diffuse glioma. *Cell.* 2016; 164(3):550–563.
18. Ritchie ME, Phipson B, Wu D, et al. limma powers differential expression analyses for RNA-sequencing and microarray studies. *Nucleic Acids Res.* 2015; 43(7):e47.
19. Liberzon A, Birger C, Thorvaldsdóttir H, Ghandi M, Mesirov JP, Tamayo P. The molecular signatures database (MSigDB) hallmark gene set collection. *Cell Syst.* 2015; 1(6):417–425.
20. Nikiforova MN, Wald AI, Melan MA, et al. Targeted next-generation sequencing panel (GlioSeq) provides comprehensive genetic profiling of central nervous system tumors. *Neuro Oncol.* 2016; 18(3):379–387.
21. Baugh EH, Ke H, Levine AJ, Bonneau RA, Chan CS. Why are there hotspot mutations in the TP53 gene in human cancers? *Cell Death Differ.* 2018; 25(1):154–160.
22. Freed-Pastor WA, Prives C. Mutant p53: one name, many proteins. *Genes Dev.* 2012; 26(12):1268–1286.
23. Gross S, Cairns RA, Minden MD, et al. Cancer-associated metabolite 2-hydroxyglutarate accumulates in acute myelogenous leukemia with isocitrate dehydrogenase 1 and 2 mutations. *J Exp Med.* 2010; 207(2):339–344.
24. Ward PS, Cross JR, Lu C, et al. Identification of additional IDH mutations associated with oncometabolite R(-)-2-hydroxyglutarate production. *Oncogene.* 2012; 31(19):2491–2498.
25. Alexandrov LB, Nik-Zainal S, Wedge DC, et al.; Australian Pancreatic Cancer Genome Initiative; ICGC Breast Cancer Consortium; ICGC MMML-Seq Consortium; ICGC PedBrain. Signatures of mutational processes in human cancer. *Nature.* 2013; 500(7463):415–421.
26. Noushmehr H, Weisenberger DJ, Diefes K, et al.; Cancer Genome Atlas Research Network. Identification of a CpG island methylator phenotype that defines a distinct subgroup of glioma. *Cancer Cell.* 2010; 17(5):510–522.
27. Guo C, Pirozzi CJ, Lopez GY, Yan H. Isocitrate dehydrogenase mutations in gliomas: mechanisms, biomarkers and therapeutic target. *Curr Opin Neurol.* 2011; 24(6):648–652.
28. Han S, Liu Y, Cai SJ, et al. IDH mutation in glioma: molecular mechanisms and potential therapeutic targets. *Br J Cancer.* 2020; 122(11):1580–1589.
29. Singh A, Gurav M, Dhanavade S, Shetty O, Epari S. Diffuse glioma - rare homozygous IDH point mutation, is it an oncogenetic mechanism? *Neuropathology.* 2017; 37(6):582–585.
30. Yang H, Ye D, Guan KL, Xiong Y. *IDH1* and *IDH2* mutations in tumorigenesis: mechanistic insights and clinical perspectives. *Clin Cancer Res.* 2012; 18(20):5562–5571.
31. Donehower LA, Soussi T, Korkut A, et al. Integrated analysis of TP53 gene and pathway alterations in the cancer genome atlas. *Cell Rep.* 2019; 28(5):1370–1384.e1375.
32. Appay R, Dehais C, Maurage CA, et al.; POLA Network. CDKN2A homozygous deletion is a strong adverse prognosis factor in diffuse malignant IDH-mutant gliomas. *Neuro Oncol.* 2019; 21(12):1519–1528.
33. Lu VM, O'Connor KP, Shah AH, et al. The prognostic significance of CDKN2A homozygous deletion in IDH-mutant lower-grade glioma and glioblastoma: a systematic review of the contemporary literature. *J Neurooncol.* 2020; 148(2):221–229.
34. Marker DF, Pearce TM. Homozygous deletion of CDKN2A by fluorescence in situ hybridization is prognostic in grade 4, but not grade 2 or 3, IDH-mutant astrocytomas. *Acta Neuropathol Commun.* 2020; 8(1):169.
35. Shirahata M, Ono T, Stichel D, et al. Novel, improved grading system(s) for IDH-mutant astrocytic gliomas. *Acta Neuropathol.* 2018; 136(1):153–166.
36. Fischer NW, Prodeus A, Gariépy J. Survival in males with glioma and gastric adenocarcinoma correlates with mutant p53 residual transcriptional activity. *Jci Insight.* 2018; 3(15):e121364.
37. Fischer M. Census and evaluation of p53 target genes. *Oncogene.* 2017; 36(28):3943–3956.
38. Bargonetti J, Prives C. Gain-of-function mutant p53: history and speculation. *J Mol Cell Biol.* 2019; 11(7):605–609.
39. van Oijen MG, Slootweg PJ. Gain-of-function mutations in the tumor suppressor gene p53. *Clin Cancer Res.* 2000; 6(6):2138–2145.
40. Lane D, Levine A. p53 Research: the past thirty years and the next thirty years. *Cold Spring Harb Perspect Biol.* 2010; 2(12):a000893.
41. Lane DP. Cancer. p53, guardian of the genome. *Nature.* 1992; 358(6381):15–16.
42. Sammons MA, Nguyen TT, McDade SS, Fischer M. Tumor suppressor p53: from engaging DNA to target gene regulation. *Nucleic Acids Res.* 2020; 48(16):8848–8869.
43. Boettcher S, Miller PG, Sharma R, et al. A dominant-negative effect drives selection of *TP53* missense mutations in myeloid malignancies. *Science.* 2019; 365(6453):599–604.
44. Willis A, Jung EJ, Wakefield T, Chen X. Mutant p53 exerts a dominant negative effect by preventing wild-type p53 from binding to the promoter of its target genes. *Oncogene.* 2004; 23(13):2330–2338.
45. Oren M, Rotter V. Mutant p53 gain-of-function in cancer. *Cold Spring Harb Perspect Biol.* 2010; 2(2):a001107.
46. Soubannier V, Stifani S. NF-κB signalling in glioblastoma. *Biomedicines.* 2017; 5(2):29.